15 June 2012 Volume 111 Number 12

AIP Journal of Applied Physics

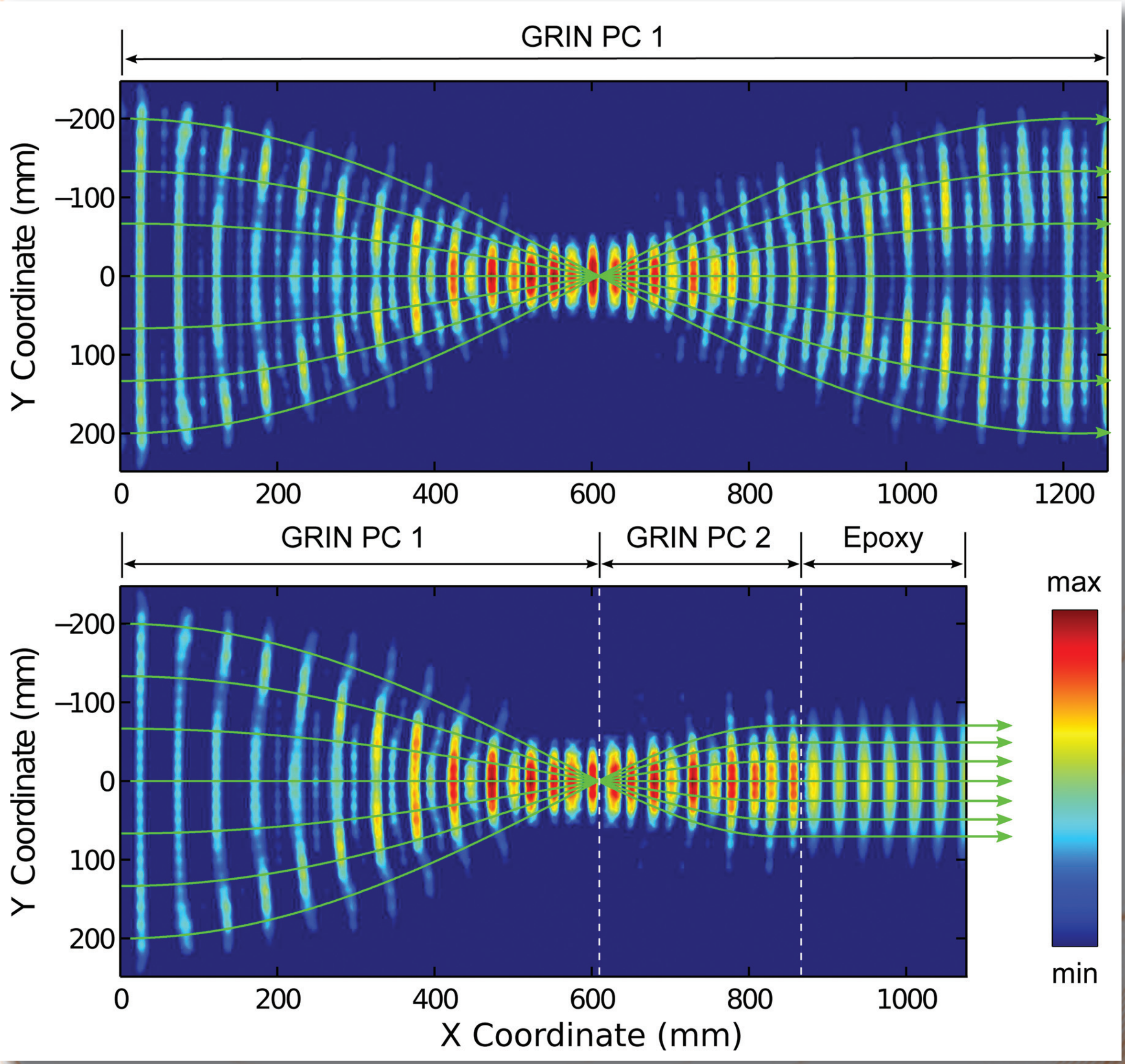

jap.aip.org

AIP | Journal of Applied Physics

Design of acoustic beam aperture modifier using gradient-index phononic crystals

Sz-Chin Steven Lin, Bernhard R. Tittmann, and Tony Jun Huang

Citation: J. Appl. Phys. **111**, 123510 (2012); doi: 10.1063/1.4729803
View online: http://dx.doi.org/10.1063/1.4729803
View Table of Contents: http://jap.aip.org/resource/1/JAPIAU/v111/i12
Published by the American Institute of Physics.

JOURNAL OF APPLIED PHYSICS **111**, 123510 (2012)

Design of acoustic beam aperture modifier using gradient-index phononic crystals

Sz-Chin Steven Lin, Bernhard R. Tittmann, and Tony Jun Huang[a)]
Department of Engineering Science and Mechanics, The Pennsylvania State University, University Park, Pennsylvania 16802, USA

(Received 23 April 2012; accepted 18 May 2012; published online 19 June 2012)

This article reports the design concept of a novel acoustic beam aperture modifier using butt-jointed gradient-index phononic crystals (GRIN PCs) consisting of steel cylinders embedded in a homogeneous epoxy background. By gradually tuning the period of a GRIN PC, the propagating direction of acoustic waves can be continuously bent to follow a sinusoidal trajectory in the structure. The aperture of an acoustic beam can therefore be shrunk or expanded through change of the gradient refractive index profiles of the butt-jointed GRIN PCs. Our computational results elucidate the effectiveness of the proposed acoustic beam aperture modifier. Such an acoustic device can be fabricated through a simple process and will be valuable in applications, such as biomedical imaging and surgery, nondestructive evaluation, communication, and acoustic absorbers. © *2012 American Institute of Physics*. [http://dx.doi.org/10.1063/1.4729803]

I. INTRODUCTION

Aperture control of an optical or acoustic beam is critical in various applications ranging from nondestructive inspection to biomedical imaging, sonoporation, and communication. Unlike the aperture of an optical beam, which can be easily reduced by an iris diaphragm and expanded by a beam expander, the aperture of an acoustic beam is difficult to modify. Owing to this complexity, there currently are no acoustic beam aperture modifiers available on the market. However, recently phononic crystals (PCs) have been introduced to enhance the control of acoustic wave propagation.[1–5] PCs are artificially engineered periodic structures that are designed to manipulate the propagation of acoustic waves. The best-known phenomenon inherent to PCs is the presence of complete phononic band gaps, within which acoustic waves cannot propagate in any direction.[6–8] PCs can also exhibit negative refraction[9,10] and self-collimation[11,12] due to the high anisotropy of the sound speed in frequency ranges close to their phononic band gaps. The versatility of devices that control acoustic wave propagation in a PC structure is further enhanced by introducing the concept of a gradient-index (GRIN).[13–17] GRIN PCs guide acoustic waves to follow a sinusoidal trajectory in the structure and thus can efficiently focus planar acoustic waves to a sub-wavelength spot or vise versa. Additionally, the wavelength-scale acoustic mirage effect in GRIN PCs can prove useful in the design of micro/nanoscale acoustic circuits.[18] Here, we further explore the functionalities of GRIN PCs by designing a GRIN PC based acoustic beam aperture modifier to efficiently vary an acoustic beam aperture, i.e., increase or decrease the beam aperture with minimum energy loss and waveform distortion. The design concept and the computational verification of the acoustic beam aperture modification are shown in Secs. II and III.

a)Author to whom correspondence should be addressed. Electronic mail: junhuang@psu.edu.

II. DESIGN CONCEPT

The proposed acoustic beam aperture modifier (Fig. 1) is composed of two butt-jointed hyperbolic-secant GRIN PCs. Each GRIN PC is a two-dimensional periodic structure composed of solid cylinders arranged in an array and embedded in a host material. Two GRIN PCs are designed in a similar fashion, but with different hyperbolic-secant gradient profiles, $n_1(y)$ and $n_2(y)$. Due to the wave speed gradient along the y-axis, normal incident waves will follow a sinusoidal propagation path through the structure. When a planar acoustic wave with an aperture of A_1 propagates in the positive x-direction, the first GRIN PC (GRIN PC A) is designed to serve as a converging lens to compress the planar wave to a focal spot located at the interface of two GRIN PCs. The second GRIN PC (GRIN PC B) then serves as a collimating lens to guide the focused acoustic wave back to be planar and parallel to the x-axis. The output acoustic beam has a smaller aperture (A_2) than that of the input acoustic beam since GRIN PC B has a sharper hyperbolic-secant refractive index profile. Likewise, the aperture of an acoustic beam propagating in the negative x-direction will be expanded by the butt-jointed GRIN PCs. In this manner, the proposed GRIN PC based device can achieve convenient beam aperture modification.

The hyperbolic-secant gradient profile of a two-dimensional GRIN PC can be obtained by different methods. In our previous study, this gradient distribution was modulated by means of the density and elastic moduli of the cylinders to tune the local wave velocity at different cylinder rows.[14,19] One can also attain such a velocity gradient by changing the diameter or shape of the cylinders.[18,20] From a practical standpoint, however, we believe that the most feasible method is to gradually tune the period of a PC consisting of equal-sized cylinders held in a homogeneous material. Our design is shown in Fig. 1, where two GRIN PCs are composed of steel cylinders of equal radii and have the same lattice constant a_x in the wave propagation direction (along

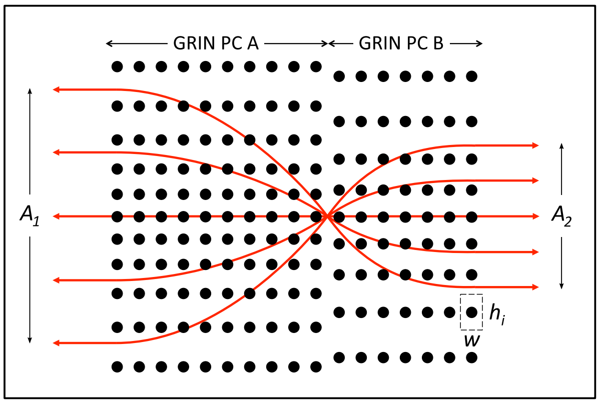

FIG. 1. Schematic of the acoustic beam aperture modifier design composed of two butt-jointed, two-dimensional GRIN PCs with different gradient profiles. The black dots represent the locations of steel cylinders, and the background material is epoxy. The aperture of a planar SV-mode BAW can be modified from wide-to-narrow or narrow-to-wide.

x-axis). The hyperbolic-secant refractive index profile in each GRIN PC is obtained by adjusting the lattice constant a_y in the transverse direction (along the y-axis). To explore the dependence of effective refractive index of a PC on its lateral lattice constant a_y, we calculate the band structures for the shear vertical (SV) mode bulk acoustic waves (BAW) of square-lattice steel/epoxy PCs with different aspect ratios ($AR = a_y/a_x = h_i/w$) using a finite-difference time-domain (FDTD) method.[21] The radii of the steel cylinders are assumed to be $r = 0.2a_x$. The material properties for steel were $\rho = 7.78\,\mathrm{g/cm^3}$, $C_L = 5.83\,\mathrm{km/s}$, and $C_T = 3.23\,\mathrm{km/s}$; and those for epoxy were $\rho = 1.14\,\mathrm{g/cm^3}$, $C_L = 2.55\,\mathrm{km/s}$, and $C_T = 1.14\,\mathrm{km/s}$, where ρ, C_L, and C_T correspond to density, longitudinal speed, and transverse speed, respectively.

Figure 2(a) shows the first two bands of the dispersion curves for SV-mode BAW propagation in six steel/epoxy PCs with different aspect ratios. Since the lattice constant a_x in the x-direction is kept constant and only the lateral lattice constant a_y is adjusted, the change in dispersion curves with varying aspect ratios is different in ΓX and ΓM orientations. With an increase in aspect ratio, the first dispersion band of the PC drops steadily along the ΓM orientation, while it remains almost unchanged along the ΓX orientation. The calculated refractive indices along the ΓX and ΓM orientations at a reduced frequency ($\Omega = \omega a_x/2\pi C$, where C is transverse wave velocity in epoxy) of 0.25 are plotted in Fig. 2(b). The refractive indices along the ΓX and ΓM orientations are defined as $n_{\Gamma X} = C/v_{\Gamma X}$ and $n_{\Gamma M} = C/v_{\Gamma M}$, respectively, where v is the group velocity. The dependence of the refractive index along the ΓM orientation ($n_{\Gamma M}$) on aspect ratio is very linear, decreasing continuously from 1.25 to 1.13 as the aspect ratio increases from 1.0 to 1.5. Conversely, the dependence of the refractive index along the ΓX orientation ($n_{\Gamma X}$) on aspect ratio is nearly negligible. The effective refractive index n_{eff} is then calculated by taking the average of $n_{\Gamma X}$ and $n_{\Gamma M}$. The lateral lattice constant a_y at each row of the GRIN PC is carefully chosen to form a hyperbolic-secant refractive index profile across the structure. Figure 2(c) shows the effective refractive index profiles of three different GRIN PCs (i.e., GRIN PC 1, GRIN PC 2, and GRIN PC 3);

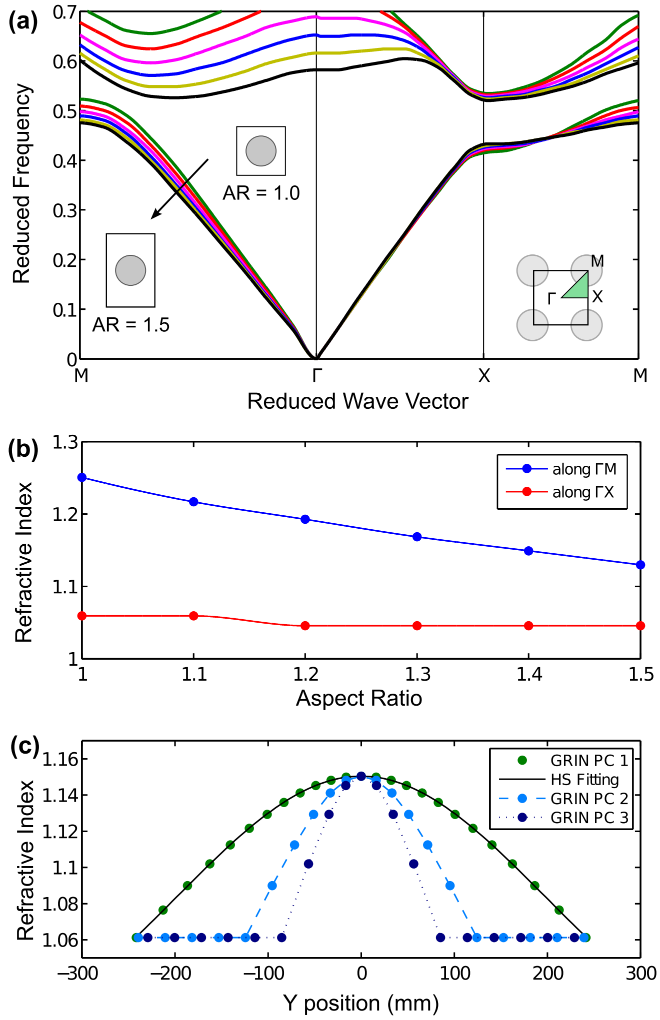

FIG. 2. (a) Band structures of rectangular-latticed steel/epoxy PC with different aspect ratios for the SV-mode BAW. (b) Refractive index of the steel/epoxy PC along ΓX and ΓM orientations against aspect ratio at reduced frequency of 0.25. (c) Effective refractive index profiles of three different GRIN PCs. Each can be fitted perfectly with a hyperbolic-secant function.

each can be fitted perfectly with a hyperbolic-secant function. As a result, each GRIN PC can be used to focus planar acoustic waves or collimate acoustic waves emitted from a point source.

III. RESULTS AND DISCUSSION

To verify the design, we simulated the acoustic wave propagation through GRIN PC 1 using the FDTD program at the design frequency of 17.78 kHz (corresponding to the reduced frequency $\Omega = 0.25$). The simulation domain used for FDTD is a two-dimensional GRIN PC that comprises 25 rows in the y-direction and 80 layers in the x-direction. The lattice spacing a_x in the x-direction is set at 16 mm and the whole domain is discretized uniformly into a density of 20 spatial grids per 8 mm. A 400-mm-long line source is placed at $x = 0$ to generate a planar SV-mode BAW by setting the body force in the out-of-plane direction (z-axis). The entire domain is surrounded by 40-grid-thick perfectly matched layers at the

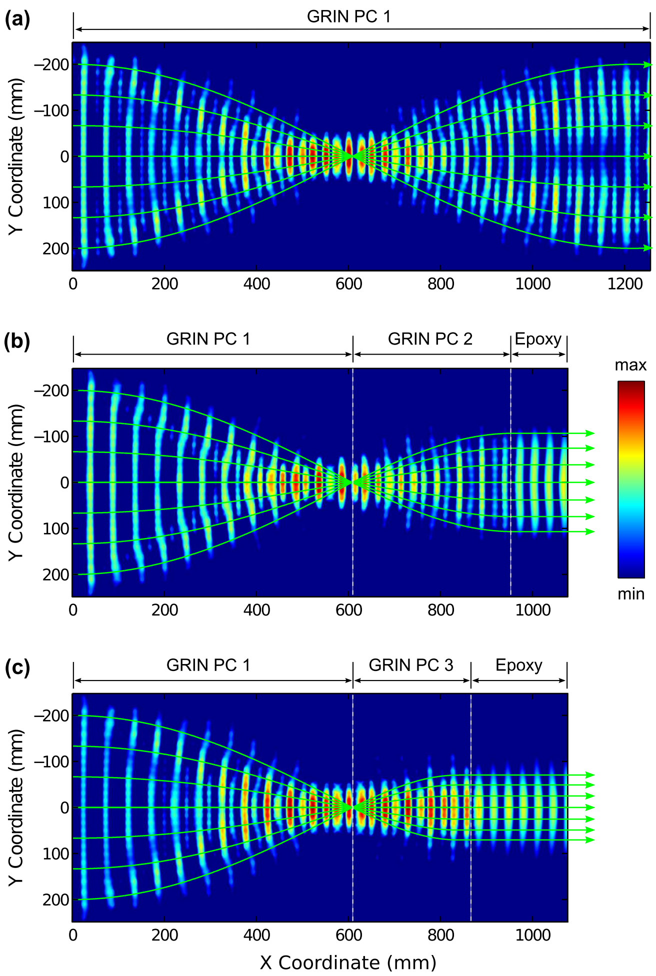

FIG. 3. FDTD-simulated acoustic wave propagation in (a) GRIN PC 1, (b) GRIN PC 1 + GRIN PC 2, and (c) GRIN PC 1 + GRIN PC 3 at the design frequency of 17.78 kHz ($\Omega = 0.25$). The line-source-width is 400 mm wide and the wave aperture at the output is (a) maintained, (b) 210 mm, and (c) 140 mm.

boundaries to avoid numerical reflections in the simulation domain. As shown in Fig. 3(a), a full-width, normally incident acoustic beam converges to a focal spot at $y = 0$, $x = 608\,\text{mm} = 38a_x$ due to the hyperbolic-secant refractive index gradient in GRIN PC 1 [Fig. 2(c)]. Beyond the focal spot, the focused beam is reconstructed to a planar wave. The overlapped beam trajectories are plotted to help one visualize the wave formation. Note that GRIN PCs can focus a normal incident beam to a single spot, and vise versa. The sharper the hyperbolic-secant gradient constructed in the GRIN PC, the shorter the focal length obtained. Hence, in design of the acoustic beam aperture modifier, we use GRIN PC 1 with a length of 608 mm ($38a_x$) as the first GRIN PC (GRIN PC A in Fig. 1) to converge the full-width (400-mm-wide) planar acoustic beam to the interface of two GRIN PCs. We then use a second GRIN PC (GRIN PC 2 or GRIN PC 3) with a sharper gradient profile in order to recover the acoustic energy in planar waves with a narrower beam aperture as portrayed in Fig. 1.

The acoustic beam aperture modification by the proposed device is numerically verified. In the proposed GRIN PC based acoustic beam aperture modifiers, the FDTD simulation demonstrated wave propagation at a reduced frequency of 0.25 as shown in Figs. 3(b) and 3(c). It can be seen from Fig. 3(b) that the full width of the acoustic beam is well focused at the interface of GRIN PC 1 and GRIN PC 2 ($x = 608$ mm) and then transmitted into GRIN PC 2. No reflection is observed at the interface due to the first columns of GRIN PC 2 being positioned exactly at the periodic frame of GRIN PC 1. The acoustic intensity at the focused spot is about 7 dB stronger than that of the incident waves. The focal zone has a -3 dB width (in the y-direction) of less than 54 mm ($3.4a_x$), which is 85% of the wavelength of the SV wave in epoxy at this frequency ($\lambda = a_x/\Omega = 4a_x$). After entering GRIN PC 2, the acoustic beam is gradually expanded and redirected to the direction parallel to the x-axis at $x = 912\,\text{mm} = 57a_x$, which is exactly the sum of the focal lengths of GRIN PC 1 ($38a_x$) and GRIN PC 2 ($19a_x$). After passing through GRIN PC 2, the transmitted acoustic beam remains collimated when propagating in epoxy. The output beam aperture at the end of the simulation domain ($x = 1060$ mm) is 210 mm, which is close to half of the width of the line source (400 mm). Therefore, this proposed beam aperture modifier achieves a 52.5% beam aperture conversion with ~90% acoustic energy conserved. In a similar design, a beam aperture modifier composed of GRIN PC 1 and GRIN PC 3 is shown in Fig. 3(c). The aperture of the output acoustic beam is measured as 140 mm at the end of the simulation domain, which is 35% of the width of the input beam aperture. The output beam has conserved 83% of the acoustic energy and is well collimated, showing no sign of either convergence or divergence. This successfully demonstrates the effectiveness of our proposed beam aperture modifier.

IV. SUMMARY

In conclusion, we propose the design, and computationally demonstrate the efficacy of an acoustic beam aperture modifier using two-dimensional gradient-index phononic crystals. The beam aperture modification is obtained by adjusting the periods of the gradient-index phononic crystals along the direction parallel to incident waves. Such aperture modifiers have the ability to change the beam aperture to 35% while conserving 83% of acoustic energy, and yet the modified beam is still well collimated. The device investigated in this work is effective and can be conveniently fabricated. Using the methodology introduced in this article, one can design acoustic beam aperture modifiers for different applications such as acoustic imaging, nondestructive evaluation, communication, and acoustic absorbers.[22]

ACKNOWLEDGMENT

We thank support from the High Performance Computing Group at the Pennsylvania State University. This work is supported by the National Institutes of Health (NIH) Director's New Innovator Award (1DP2OD007209-01), the National Science Foundation, and the Penn State Center for Nanoscale Science (MRSEC).

[1]J. Sánchez-Pérez, D. Caballero, R. Mártinez-Sala, C. Rubio, J. Sánchez-Dehesa, F. Meseguer, J. Llinares, and F. Gálvez, Phys. Rev. Lett. **80**, 5325–5328 (1998).
[2]F. Montero de Espinosa, E. Jiménez, and M. Torres, Phys. Rev. Lett. **80**, 1208–1211 (1998).
[3]J. O. Vasseur, P. Deymier, B. Chenni, B. Djafari-Rouhani, L. Dobrzynski, and D. Prevost, Phys. Rev. Lett. **86**, 3012–3015 (2001).
[4]R. Sainidou, N. Stefanou, and A. Modinos, Phys. Rev. B **66**, 212301 (2002).
[5]F. Wu, Z. Hou, Z. Liu, and Y. Liu, J. Phys. D: Appl. Phys. **35**, 162 (2002).
[6]T.-T. Wu, Z.-G. Huang, and S.-C.S. Lin, Phys. Rev. B **69**, 094301 (2004).
[7]V. Laude, Y. Achaoui, S. Benchabane, and A. Khelif, Phys. Rev. B **80**, 092301 (2009).
[8]M. Oudich, Y. Li, B. M. Assouar, and Z. Hou, New J. Phys. **12**, 083049 (2010).
[9]M. Ke, Z. Liu, C. Qiu, W. Wang, J. Shi, W. Wen, and P. Sheng, Phys. Rev. B **72**, 064306 (2005).
[10]J. Pierre, O. Boyko, L. Belliard, J. O. Vasseur, and B. Bonello, Appl. Phys. Lett. **97**, 121919 (2010).
[11]A. Cicek, O. A. Kaya, and B. Ulug, J. Phys. D: Appl. Phys. **44**, 205104 (2011).
[12]J. Shi, S.-C.S. Lin, and T. J. Huang, Appl. Phys. Lett. **92**, 111901 (2008).
[13]D. Torrent and J. Sánchez-Dehesa, New J. Phys. **9**, 323–323 (2007).
[14]S.-C.S. Lin, T. J. Huang, J.-H. Sun, and T.-T. Wu, Phys. Rev. B **79**, 094302 (2009).
[15]T. P. Martin, M. Nicholas, G. J. Orris, L.-W. Cai, D. Torrent, and J. Sanchez-Dehesa, Appl. Phys. Lett. **97**, 113503 (2010).
[16]S. Peng, Z. He, H. Jia, A. Zhang, C. Qiu, M. Ke, and Z. Liu, Appl. Phys. Lett. **96**, 263502 (2010).
[17]T.-T. Wu, Y.-T. Chen, J.-H. Sun, S.-C.S. Lin, and T. J. Huang, Appl. Phys. Lett. **98**, 171911 (2011).
[18]S.-C.S. Lin and T. J. Huang, J. Appl. Phys. **106**, 053529 (2009).
[19]S.-C.S. Lin, B. R. Tittmann, J.-H. Sun, T.-T. Wu, and T. J. Huang, J. Phys. D: Appl. Phys. **42**, 185502 (2009).
[20]A. Climente, D. Torrent, and J. Sanchez-Dehesa, Appl. Phys. Lett. **97**, 104103 (2010).
[21]J.-H. Sun and T.-T. Wu, Phys. Rev. B **74**, 174305 (2006).
[22]A. Climente, D. Torrent, and J. Sánchez-Dehesa, Appl. Phys. Lett. **100**, 144103 (2012).